Plasmonics (2014) 9:1431–1437
DOI 10.1007/s11468-014-9760-x

Theoretical Analysis of Plasmon-Induced Transparency in Ring-resonators Coupled Channel Drop Filter Systems

Shiping Zhan · Hongjian Li · Guangtao Cao · Zhihui He · Boxun Li · Hui Xu

Received: 6 May 2014 / Accepted: 16 July 2014 / Published online: 27 July 2014

Abstract The plasmon-induced transparency (PIT) in ring-resonators coupled channel drop filter (CDF) systems is investigated theoretically and numerically in this paper. A coupled mode theory-based transfer matrix method (CMT-TMM) is introduced owning to the symmetric and evanescent coupling, which is confirmed by the finite-difference time-domain (FDTD) simulation results. The drop waveguide provides the necessary optical feedback for the interference effect in realizing the PIT, and a new way for adjusting PIT effect in a fixed structure is also given. Finally, the phase and the group dispersion in the transparency window are discussed for investigating the slow light effect in our systems, and a group index of ~22 is obtained. The proposed plasmonic systems possess both the slow light and the dropping properties and may have potential and flexible applications in fundamental research of integrated plasmonic devices.

Keywords Nanoplasmonics · Coupled mode analysis · Feedback · Integrated plasmonic devices · Plasmon-induced transparency

Introduction

Electromagnetically induced transparency (EIT) is the result of a quantum destructive interference in atomic system [1–3]. Recently, analogue of EIT in a non-atomic way attracts researchers' attentions due to the soft experiment limitations comparing with the quantum one but possessing similar properties, such as slow light effect [4–7].

Plasmon-induced transparency (PIT), usually considered as a plasmonic analogue of EIT owning to the extraordinary capabilities of surface plasmon polaritons (SPPs), is widely discussed [8–19], such as in metamaterials [8–10], gratings [11–13], metal-insulator-metal (MIM) waveguide systems [14–17]. MIM waveguide system interests people because of its advantages of easy technical fabrication and supporting the manipulation as well as strong confinement of light on a subwavelength scale. Huang et al. [14] and Wang et al. [15] reported the PIT in MIM waveguide; Han et al. studied the PIT with detuned Fabry-Perot resonators in a plasmonic system [16]. Nevertheless, these current researches mainly focus on the direct coupling between waveguide and resonators, for example, stubs or cavities. In such resonators, the energy escapes into the bus waveguide in both forward and backward directions leaving the reflected wave also in the bus waveguide [15–17], which is not convenient for the extraction and separation of some specific waves, and may also limit the multifunctional applications of integrated plasmonic devices. The ring resonator supports whispering gallery modes due to the total intrinsic reflection as well as the nearly eliminated bending loss [20] and can be considered as a useful element in integrated plasmonic device. Meanwhile, the common investigations of PIT are usually based on asymmetric coupling; studies on symmetric coupling are still not widely reported [21, 22]. Here, we propose a design of plasmonic ring-resonator coupled channel drop filter (CDF) system, which possesses both the symmetric coupling and filter property, can ideally satisfy those requirements by doing some specific designs [20]. For better understanding of the optical response in plasmonic systems, some theoretical models are also established [14, 23, 24]. However, systematic theoretical analysis of PIT in ring-resonators coupled CDF system is still not particularly discussed, which may be beneficial for realizing

S. Zhan · H. Li (✉) · Z. He · B. Li · H. Xu
College of Physics and Electronics, Central South University, Changsha 410083, People's Republic of China
e-mail: lihj398@126.com

H. Li · G. Cao
College of Materials Science and Engineering, Central South University, Changsha 410083, China

the mechanism and insight as well as the fundamental applications of PIT.

In this work, we report a theoretical analysis of plasmon-induced transparency in the ring-resonators coupled CDF systems. A coupled mode theory-based transfer matrix method (CMT-TMM) is introduced. The established theoretical model is well verified by the finite-difference time-domain (FDTD) simulations. It is found that the drop waveguide plays a key role in providing the optical feedback for the PIT effect, and we also provide a new way for adjusting the PIT effect in a fixed structure. Finally, the phase and the group dispersion in the transparency window are also discussed for the slow light effect, and a group index of ~22 is achieved in the proposed plasmonic systems.

Structure Model and Simulation

Figure 1 illustrates the schematic diagram of the proposed ring-resonators coupled CDF systems. Plasmonic resonators labeled from 1 to n are placed between the two parallel MIM waveguides W1 and W2, both of which have the same width w= 50 nm. When an incident pulse goes into W1 from the left port, the SPP wave generates in the metal-dielectric interface and can be coupled into the resonator due to the satisfaction of resonance condition [16]. Here, the ring-resonator is considered supporting a traveling-wave mode and the mode decays in a clockwise direction into W1 and W2. The distance d between the waveguides and the rings is set to be 20 nm which guarantees an evanescent coupling. The background metal is chosen to be silver (Ag), of which the frequency dependent permittivity is approximately defined by the Drude model [25] as

$$\varepsilon(\omega) = 1 - \frac{\omega_p^2}{\omega^2 + \gamma_p^2} + i\frac{\omega_p^2\gamma_p^2}{\omega\left(\omega^2 + \gamma_p^2\right)}. \quad (1)$$

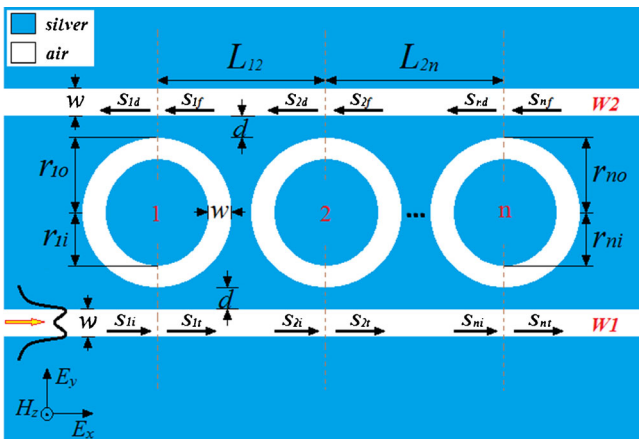

Fig. 1 Diagram of channel drop filter systems. r_{no} and r_{ni} are the outer and inner radiuses of the nth ring-resonator, respectively. $L_{(n-1)n}$ represents the core-core distance between the n-1th and nth rings, while the red dashed lines in middle are the reference planes for ring-resonators

where ω_p=1.38×10^{16} s^{-1} is the bulk plasmon frequency, ω stands for the angle frequency of the incident wave, and γ_p= 2.37×10^{13} s^{-1} represents the damping rate [25]. The spacer colored white is air with permittivity ε_d=1 for simplicity. The characteristic spectral responses of the chosen structures are performed by the two-dimensional FDTD simulation [26]. The spatial and temporal steps are set as Δx=Δy=2.5 nm and Δt=Δx/2c (c is the velocity of light in vacuum), respectively.

Theoretical and Numerical Analysis

We first deduce the CMT-TMM for our proposed structure. For the single ring-resonator coupled CDF system, the transmission and the drop spectra exhibit a resonance dip and a peak, respectively [20]. For two or more ring-resonators coupled systems in Fig. 1, however, the dropped wave from the nth ring will be coupled back into the n-1th ring through the top waveguide. The total amplitude decay of the nth ring-resonator can be described as $1/\tau_n = 1/\tau_{no} + 1/\tau_{ne} + 1/\tau_{nd} = 1/\tau_{no} + 2/\tau_{ne}$, where $1/\tau_{no} = \gamma_{no} = \pi c/\lambda_n Q_{no}$ and $2/\tau_{ne} = \gamma_{ne} = \pi c/\lambda_n Q_{ne}$ are decay rates corresponding to the intrinsic loss effect and the power coupled externally to the transmitted and the output waveguides, respectively. The last equal sign for $1/\tau_n$ results from the symmetric design in our configuration. Q_{no} and Q_{ne} are the related quality factors (QF) which characterize the internal and the coupling loss, respectively. The relationship among Q_{nt}, Q_{no}, and Q_{ne} for the nth ring-resonator is $1/Q_{nt} = 1/Q_{no} + 1/Q_{ne}$, where Q_{nt} is the total quality factor of the single nth ring in the coupled system and can be evaluated from the formula that $Q_{nt} = \lambda_n/\Delta\lambda_n$, where λ_n is the resonance wavelength and $\Delta\lambda_n$ is the full width of half maximum (FWHM) of the transmission spectrum for the single nth ring-resonator coupled CDF system. Q_{no} is the intrinsic quality factor and can be obtained from [27] Q_o=Re(n_{eff})/2Im(n_{eff}).

Thus, the mode amplitude a_n (n=1, 2,…, N, N is an integer) of the nth resonator can be described by a temporal coupled harmonic oscillator model as

$$-i\omega a_n = \left(-i\omega_n - \frac{1}{\tau_{no}} - \frac{2}{\tau_{ne}}\right)a_n + \sqrt{\frac{2}{\tau_{ne}}}\left(S_{ni} + S_{(n+1)d}\right) \quad (2)$$

$$S_{nt} = S_{ni} - \sqrt{\frac{2}{\tau_{ne}}}a_n, \quad S_{nd} = S_{nf} - \sqrt{\frac{2}{\tau_{ne}}}a_n, \quad (3)$$

where ω is the angular frequency of the input optical pulse, ω_n is the resonance frequency, and S_{ni}, S_{nd}, S_{nt}, and S_{nf} are

amplitudes describing the incident, dropped, transmitted, and feedback wave of the nth ring cavity, respectively.

For a single ring-resonator coupling situation, S_{nf} is zero due to the fact that no feedback wave from the $n+1$th ring and the optical pulse is only inputted from the left port of the W1. So the complex transmission t_n (S_{nt}/S_{ni}) and drop coefficient d_n (S_{nd}/S_{ni}) can be derived from Eqs. 2 and 3 as follows: $t_n=(i(\omega_n-\omega)+\gamma_{no})/(i(\omega_n-\omega)+\gamma_n)$, $d_n=-\gamma_{ne}/(i(\omega_n-\omega)+\gamma_n)$, where $\gamma_n=\gamma_{ne}+\gamma_{no}$. The transmission T and phase shift θ can be calculated as $T=abs(t)^2$ and $\theta=arg(t)$, respectively. Here, t is the total transmission coefficient of the system. Then the transfer matrix of the waves between the left and right ports for the nth ring coupled CDF system can be given by

$$\begin{bmatrix} S_{nf} \\ S_{nt} \end{bmatrix} = \begin{bmatrix} -d_n/t_n & 1/t_n \\ 1+d_n/t_n & d_n/t_n \end{bmatrix} \begin{bmatrix} S_{ni} \\ S_{nd} \end{bmatrix} \quad (4)$$

When the incoming wave travels in the n ring-resonators coupled systems, some relationships should be satisfied as $S_{(n-1)f}=S_{nd}exp(i\varphi_{(n-1)n})$ and $S_{ni}=S_{(n-1)t}exp(i\varphi_{(n-1)n})$ in the steady state. Here, $\varphi_{(n-1)n}=\mathrm{Re}(\beta_{spp})L_{(n-1)n}=2\pi\mathrm{Re}(n_{eff})L_{(n-1)n}/\lambda$ represents the phase difference between the reference planes of the n-1th and the nth ring-resonators during the wave propagating in W1 and W2. The complex wave vector β_{spp} and effective refractive index n_{eff} in a MIM waveguide with a width w can be obtained from Ref. [16].

Then we obtain the transfer matrixes for the single ring-resonator coupled CDF system and the phase difference from the above analysis as

$$M_n = \begin{bmatrix} -d_n/t_n & 1/t_n \\ 1+d_n/t_n & d_n/t_n \end{bmatrix}, P_{(n-1)_n} = \begin{bmatrix} 0 & e^{i\varphi_{(n-1)n}} \\ e^{-i\varphi_{(n-1)n}} & 0 \end{bmatrix} \quad (5)$$

Finally, the relation between the wave amplitudes in the left and the right ports of the entire n ring-resonators coupled CDF systems can be given as

$$\begin{bmatrix} S_{nf} \\ S_{nt} \end{bmatrix} = M_n P_{(n-1)n} M_{(n-1)} P_{(n-2)(n-1)} M_{(n-2)} \ldots M_2 P_{12} M_1 \begin{bmatrix} S_{1i} \\ S_{1d} \end{bmatrix} \quad (6)$$

To verify the deduced TMM in the former section, we first analyze the simulation results in the two ring-resonators coupled systems. The inner radiuses for the two coupled rings are set as r_{1i}=150 nm and r_{2i}=144 nm while the outer radiuses r_{no} (n=1, 2) are 200 nm for both and keep constant in the following discussion. The distance d between the two waveguides and the rings is 20 nm for a symmetric coupling. Figure 2a–d are the transmission spectra for different L_{12}. A transmission peak located at 529.1 nm while two dips at 517.2 and 539 nm are observed in the transmission spectra, which reveal the typical EIT-like phenomenon in non-atomic systems [14–17]. The quality factors $Q_{1(2)t}$ and $Q_{1(2)o}$ are estimated as 82.8 (53.4) and 464 (498) for ring 1 (2) in the theoretical fitting, respectively. Those give the theoretical profiles of transmission spectra through $T=|S_{2t}/S_{1i}|^2=|t_1t_2/(\exp(-i\varphi_{12})-d_1d_2\exp(i\varphi_{12}))|^2$ by combining Eqs. 5 and 6, shown as blue circles, which match well with the simulation results as red solid lines. The black arrow marked M represents the maximum transmission and indicates that the resonance condition is satisfied when L_{12}=580 nm. The physical mechanism can be described as that the inputted wave enters from the left port of W1, and then divides into S_{1t} and S_{1d} when it passes through the first ring-resonator. Meanwhile, the dropped wave S_{2d} from the second ring can be treated as a feedback and couples back into the former one through W2. The whole optical process in our ring-resonators coupled CDF systems is similar to the Fabry-Perot model with frequency dependent end-mirror reflectivities [17]. Figure 2e depicts the transmission at 529.1 nm as a function of different L_{12}. As the red dots shown, the transmission increases firstly as L_{12} increases from 500 to 580 nm while decreases as it further increases from 580 to 680 nm when the top MIM waveguide W2 exists. But if we remove W2, the feedback coupling from the dropped wave vanishes accordingly which makes the transmission as a constant of nearly 0.82 as L_{12} increases, shown as black squares. Therefore, we can conclude that the formation mechanism of the PIT effect in the proposed systems works as our theoretical analysis described above and the drop channel W2 plays an important role in providing the necessary optical feedback for the interference effect in realizing the PIT effect. Figure 2f shows the evolution of transmission spectrum with varied L_{12} where a non-monotonic change of transmission can be clearly observed, which provides a further support of our former analysis on Fig. 2e.

Simulation and theoretical transmission spectra for different wavelength detuning δ_λ are also plotted in Fig. 3a–d, here, r_{2i} varies from 140 to 149 nm while r_{1i} keeps 150 nm. The coupling distance L_{12} is 580 nm as a constant in this section. Figure 3b shows a nearly symmetric profile in the transparency window due to the fact that the resonance condition is satisfied here and φ_{12} equals 3π at 529.1 nm, while unsatisfied for the other threes at 521.4, 533.8, and 535.4 nm, therefore, leading to the less symmetry in Fig. 3a, c, d. Similar results can also be found in the plasmonic antennas coupled silicon waveguide [28]. During the theoretical fitting, Q_{2t} are estimated as 60, 53.4, 74.5, and 78 for Fig. 3a–d, respectively. The phase shift for each δ_λ is given in Fig. 3e. As δ_λ decreases, the phase shift in the transparency window turns to be steeper and may result in a higher group index n_g from $n_g=c/v_g=c/H\cdot\tau_g=c/H\cdot(d\theta(\omega)/(d\omega))$, where v_g is the group velocity of the pulse, τ_g is the delay time, and the phase shift $\theta(\omega)$ is the function of angular frequency ω; H=1,200 nm is the length of the plasmonic system. The maximum group index and the transmission in the transparency windows for different r_{2i} are plotted in

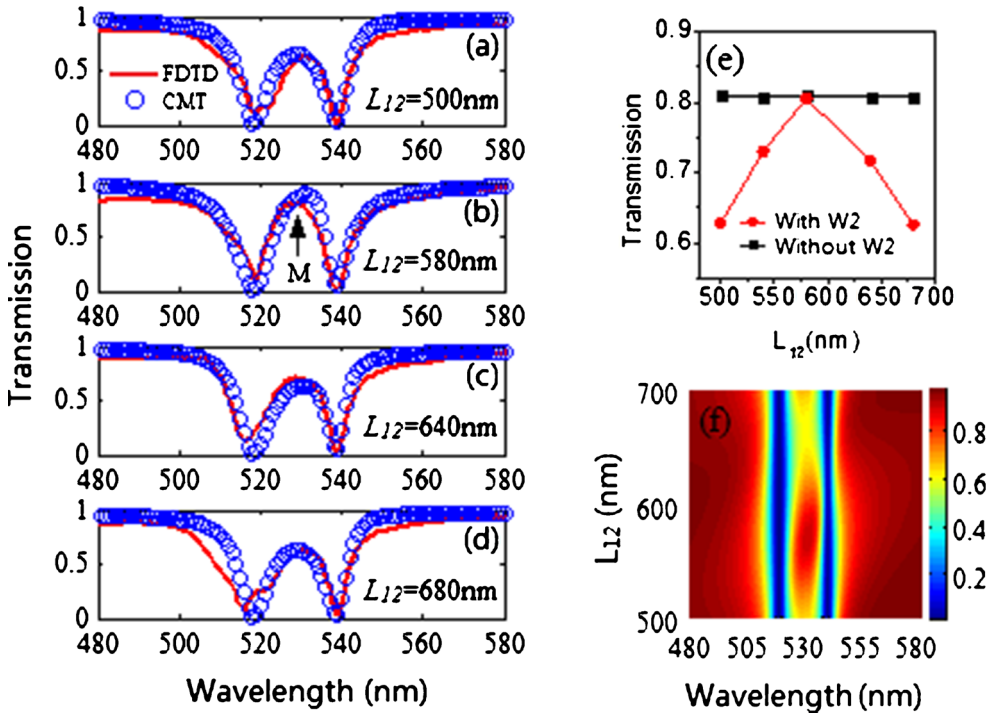

Fig. 2 Transmission spectra of the structure with different L_{12} **a** 500 nm, **b** 580 nm, **c** 640 nm, and **d** 680 nm. The *circles* are the theoretical results, and the *solid curves* are the simulation ones. **e** Transmission at 529.1 nm as a function of different L_{12}. **f** Evolution of transmission spectrum with varied L_{12}

Fig. 3f. It is observed that as δ_λ decreases, the group index shows an ascending trend and achieves ~22 when r_{2i}= 149 nm, which indicates a slow light effect in our plasmonic systems. The transmission max, however, shows an opposite changing as δ_λ decreases but guarantees a higher quality factor in the transparency window. The quality factors of the transparency windows are estimated as 16, 40.6, 50, 111.2, and 184.6 for r_{2i} equaling 140, 144, 146, 148, and 149 nm, respectively. Therefore, adjusting the inner radius of ring 2 in the coupled systems offers a convenient way to manipulate the

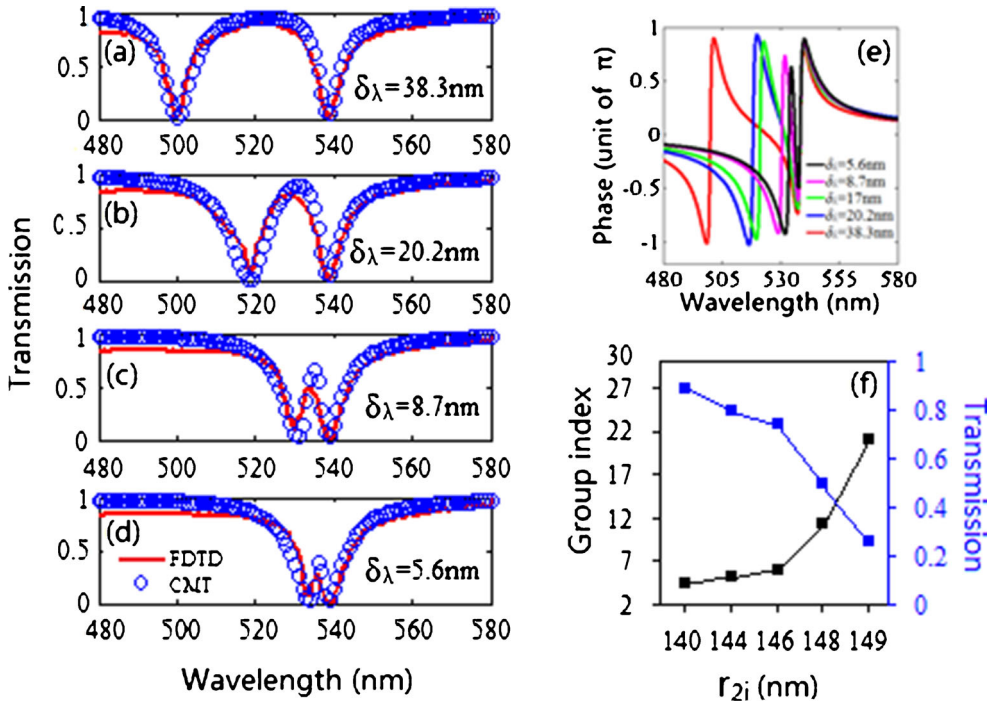

Fig. 3 Transmission spectra of the structure with varied wavelength detuning δ_λ, and the inner radius for ring 2 is set as **a** 140 nm, **b** 144 nm, **c** 148 nm, **d** 149 nm, and 146 nm (not given for brevity). The *circles* are the theoretical results, and the *solid curves* are the simulation ones. **e** The corresponding phase dispersion $\theta(\omega)$, **f** group index n_g and the transmission of transparency peak as a function of r_{2i}

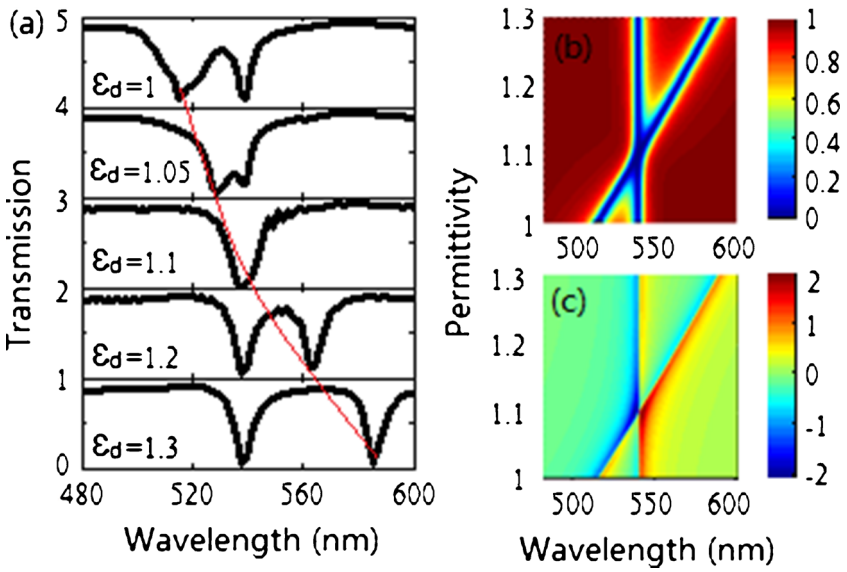

Fig. 4 **a** Simulation spectra with r_{1i}=150 nm, r_{2i}=144 nm, and L_{12}=680 nm while the permittivity ranges from 1 to 1.3. **b** Evolution of transmission spectrum with varied ε_d. **c** Evolution of transmission phase shift in unit of π

group index and quality factor in the transparency window, which may provide some simple applications in slow light devices.

Additionally, we embed material with varied permittivity ε_d in ring 2 and discuss the optical response. Figure 4a shows the simulation transmission spectra with r_{1i}=150 nm, r_{2i}=144 nm, and L_{12}=680 nm while the permittivity ε_d ranges from 1 to 1.3. It is known that a higher refractive index in resonator can result in a longer resonance wavelength through the resonance condition [29]. Here in our two ring-resonators coupled CDF systems, the first transmission dip at 518 nm is attributed to ring 2 while the second one at 539 nm is attributed to ring 1 when ε_d=1. As ε_d increases, an apparent redshift for the first dip is observed and the moving track is also marked as a red curve, while the second one almost keeps still. When ε_d=1.1, the two resonance modes of ring 1 and 2 can be treated as degenerate; therefore, the spectrum shows only one transmission dip at 539 nm. This provides a new way for the realization of tuning PIT in a fixed structure design without changing the structure size, which can be theoretically beneficial for the integration of plasmonic devices. The theoretical transmission evolution is also depicted in Fig. 4b, which is in accordance with the simulation results. Here, we assume that Q_{t2} keeps proportional with ε_d for an approximation due to the fact that λ_2 increases while $\Delta\lambda_2$ nearly maintains the same for an increasing ε_d [30]. Figure 4c shows the

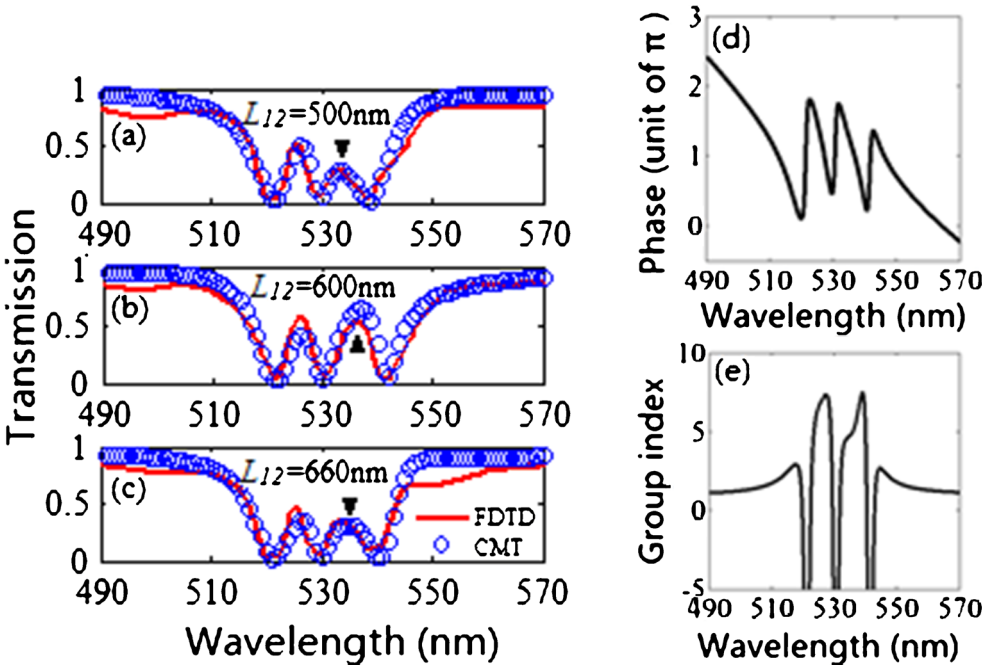

Fig. 5 **a**–**c** The transmission spectra of the three rings coupled systems with r_{1i}=150 nm, r_{2i}=148 nm, r_{3i}=146 nm, and L_{23}=600 nm while L_{12}=500, 600, and 660 nm, respectively. The *circles* are theoretical results and the *solid curves* are simulation ones. **d**–**e** are the related transmission phase shift and group index with L_{12}=L_{23}=600 nm, respectively

related transmission phase shift in unit of π. We can observe that the phase shift becomes steep around ε_d=1.1, which agrees with the above analysis and may lead to a slow light effect.

For the further confirmation of the derived theoretical formulas in the former part, we finally investigate the PIT effect in three ring-resonators coupled CDF systems briefly. Figure 5a–c shows the optical response of the coupled systems with r_{1i}=150 nm, r_{2i}=148 nm, r_{3i}=146 nm, and L_{23}=600 nm while L_{12}=500, 600, and 660 nm, respectively. Two transparency windows are observed between 521 and 539 nm. The first transmission peak attributes to the phase coupled PIT between rings 2 and 3, and the second one is due to that between rings 1 and 2. Here, we verify this understanding by changing L_{12}, while L_{23} keeps the same for comparison. As discussed above, the coupling between two ring-resonators is mainly attributed to the phase difference between their reference planes. Therefore, a varied transmission peak located at 535 nm and marked as black triangle is observed relating to L_{12}, while the first transmission peak nearly maintains the same because of the constant L_{23}. The quality factor Q_{t3} and Q_{o3} for ring 3 are estimated as 63 and 488 in the theoretical fitting, and it is also observed that the theoretical profiles show good agreement with the simulation results. The transmission phase shift dispersion for the structure in Fig. 5b is abstracted as Fig. 5d, and the corresponding group index is also calculated with H= 1800 nm, shown in Fig. 5e. The maximum group index is close to 8 for each transparency window. It is found that our theoretical model also provides good realization on this multi-PIT effect in three ring-resonators coupled plasmonic systems. All the results observed and discussed here corroborate that we have proposed the theoretical and numerical understandings of the plasmon-induced transparency in ring-resonators coupled CDF systems.

Conclusion

In summary, the plasmon-induced transparency effect in the ring-resonators coupled CDF systems has been theoretically and numerically investigated. The properly introduced CMT-TMM gives clear understandings of PIT in the coupled plasmonic systems, which is confirmed by the FDTD simulations. It is found that the drop waveguide plays a key role in providing the optical feedback for the PIT effect, and the flexible tuning of PIT in a fixed structure is obtained in a simple way. The steep phase and the group dispersion in transparency window guarantee a slow light effect, and a group index of ~22 is achieved in this plasmonic structure. All these findings suggest the valuable potential of our proposed plasmonic design to fundamental researches and applications in the area of plasmonic devices.

Acknowledgments This work was funded by the Fundamental Research Funds for the Central Universities of Central South University under Grant No. 72150050429 and 2012zzts007, the Research Fund for the Doctoral Program of Higher Education of China under Grant No. 20100162110068, and the National Natural Science Foundation of China under Grant No. 61275174.

References

1. Mirza AB, Singh S (2012) Wave-vector mismatch effects in electromagnetically induced transparency in Y-type systems. Phys Rev A 85(5):053837
2. Laupretre T, Kumar S, Berger P, Faoro R, Ghosh R, Bretenaker F, Goldfarb F (2012) Ultranarrow resonance due to coherent population oscillations in a Λ-type atomic system. Phys Rev A 85(5):051805(R)
3. Raymond Ooi CH, Tan KS (2013) Controlling double quantum coherence and electromagnetic induced transparency with plasmonic metallic nanoparticle. Plasmonics 8(2):891–898
4. Chen JX, Wang P, Chen CC, Lu YH, Ming H, Zhan QW (2011) Plasmonic EIT-like switching in bright-dark-bright plasmon resonators. Opt Express 19(7):5970–5978
5. Xiao YF, Zou XB, Jiang W, Chen YL, Guo GC (2007) Analog to multiple electromagnetically induced transparency in all-optical drop-filter systems. Phys Rev A 75(6):063833
6. Chen JJ, Li Z, Yue S, Xiao JH, Gong QH (2012) Plasmon-induced transparency in asymmetric T-shape single slit. Nano Lett 12(5): 2494–2498
7. Cao GT, Li HJ, Zhan SP, Xu HQ, Liu ZM, He ZH, Wang Y (2013) Formation and evolution mechanisms of plasmon-induced transparency in MDM waveguide with two stub resonators. Opt Express 21(7):9198–9205
8. Li Z, Ma Y, Huang R, Singh R, Gu J, Tian Z, Han J, Zhang W (2011) Manipulating the plasmon-induced transparency in terahertz metamaterials. Opt Express 19(9):8912–8919
9. Singh R, Al-Naib IA, Yang Y, Chowdhury DR, Cao W, Rockstuhl C, Ozaki T, Morandotti R, Zhang W (2011) Observing metamaterial induced transparency in individual Fano resonators with broken symmetry. Appl Phys Lett 99(20):201107
10. Tassin P, Zhang L, Koschny T, Economou EN, Soukoulis CM (2009) Planar designs for electromagnetically induced transparency in metamaterials. Opt Express 17(7):5595–5605
11. Tang B, Dai L, Jiang C (2011) Electromagnetically induced transparency in hybrid plasmonic-dielectric system. Opt Express 19(2):628–637
12. Jia S, Wu YM, Wang XH, Wang N (2014) A subwavelength focusing structure composite of nanoscale metallic slits array with patterned dielectric substrate. IEEE Photonics J 6(1):4800108
13. Gan QQ, Fu Z, Ding YJ, Bartoli FJ (2008) Ultrawide bandwidth slow-light system based on THz plasmonic graded metallic grating structures. Phys Rev Lett 100(25):256803
14. Huang Y, Min CJ, Veronis G (2011) Subwavelength slow-light waveguides based on a plasmonic analogue of electromagnetically induced transparency. Appl Phys Lett 99(14):143117
15. Wang GX, Lu H, Liu XM (2012) Dispersionless slow light in MIM waveguide based on a plasmonic analogue of electromagnetically induced transparency. Opt Express 20(19):20902–20907
16. Han ZH, Bozhevolnyi SI (2011) Plasmon-induced transparency with detuned ultracompact Fabry-Perot resonators in integrated plasmonic devices. Opt Express 19(4):3251–3257

17. Lu H, Liu XM, Mao D (2012) Plasmonic analog of electromagnetically induced transparency in multi-nanoresonator-coupled waveguide systems. Phys Rev A 85(5):053803
18. He YR, Zhou H, Jin Y, He SL (2011) Plasmon induced transparency in a dielectric waveguide. Appl Phys Lett 99(4):043113
19. Liu JT, Xu BZ, Zhang J, Song GF (2013) Double plasmon-induced transparency in hybrid waveguide-plasmon system and its application for localized plasmon resonance sensing with high figure of merit. Plasmonics 8(2):995–1001
20. Manolatou C, Khan MJ, Fan SH, Villeneuve PR, Haus HA, Joannopoulos JD (1999) Coupling of modes analysis of resonant channel add–drop filters. IEEE J Quantum Electron 35(9):1322–1331
21. Liu XJ, Gu JQ, Singh RJ, Ma YF, Zhu J, Tian Z, He MX, Han JG, Zhang WL (2012) Electromagnetically induced transparency in terahertz plasmonic metamaterials via dual excitation pathways of the dark mode. Appl Phys Lett 100(13):131101
22. Liu ZM, Li HJ, Zhan SP, Cao GT, Xu HQ, Yang H, Xu XK (2013) PIT-like effect in asymmetric and symmetric C-shaped metamaterials. Opt Mater 35(5):948–953
23. Li Q, Wang T, Su YK, Yan M, Qiu M (2010) Coupled mode theory analysis of mode-splitting in coupled cavity system. Opt Express 18(8):8367–8382
24. Pannipitiya A, Rukhlenko ID, Premaratne M, Hattori HT, Agrawal GP (2010) Improved transmission model for metal-dielectric-metal plasmonic waveguides with stub structure. Opt Express 18(6):6191–6204
25. Palik ED (ed) (1985) Handbook of optical constants of solids. Academic, Boston
26. Taflove A, Hagness SC (2005) Computational electrodynamics: the finite-difference time-domain method, 3rd edn. Artech, House, Boston
27. Han ZH (2010) Ultracompact plasmonic racetrack resonators in metal-insulator-metal waveguides. Photonic Nanostruct 8(3):172–176
28. Kekatpure RD, Barnard ES, Cai WS, Brongersma ML (2010) Phase-coupled plasmon-induced transparency. Phys Rev Lett 104(24):243902
29. Tian M, Lu P, Chen L, Lv C, Liu DM (2011) A subwavelength MIM waveguide resonator with an outer portion smooth bend structure. Opt Commun 284(16–17):4078–4081
30. Wang GX, Lu H, Liu XM, Mao D, Duan LN (2011) Tunable multi-channel wavelength demultiplexer based on MIM plasmonic nano-disk resonators at telecommunication regime. Opt Express 19(4):3513–3518